JOURNAL OF THERMOPHYSICS AND HEAT TRANSFER
Vol. 35, No. 3, July–September 1998

Near-Isothermal Regenerator: Complete Thermal Characterization

Luc Bauwens*
University of Calgary, Calgary, Alberta T2N 1N4, Canada

Near-isothermal analysis of thermal regenerators used in Stirling and pulse-tube refrigerators is based upon realistic assumptions for temperatures above 10 K. The flow passages are small compared to the conductive heat penetration depth in the gas and the thermal mass of the matrix is large compared to that of the gas. The analysis shows that the oscillating flow includes a thermoacoustic effect, so that the enthalpy flux is not equivalent to a heat flux leaking across a temperature difference. An evaluation of the entropy sources allows for splitting the enthalpy flux into a reversible component and a loss. This one-dimensional model, applicable to arbitrary matrix topologies, uses an empirical convection coefficient for heat transfer. To assess its validity, results for a laminar, constant Nusselt number are compared with two-dimensional results for a tubular regenerator based upon the exact physics of transverse heat transfer. The comparison shows that empirical convection coefficients yield incorrect results and that the error increases with the pressure amplitude.

Nomenclature

a = dimensionless parameter of order unit, $\tau\alpha_m/\varepsilon\delta L^2$
c_p = specific heat at constant pressure
d = mesh size
$\dot{H}$ = enthalpy flux through the regenerator
L = regenerator length
$\dot{m}$ = mass flow rate
Nu = Nusselt number, based upon mesh size
p = pressure
Q = heat in/out
r = ratio of net gas-filled cross section/cross section filled with regenerator material
$\dot{S}(x)$ = entropy flux over one period, at location x, $\int_0^1 \dot{m}s\ \mathrm{d}t$
s = specific entropy
T = temperature
t = time
W = piston work
x = position
α = heat diffusivity
γ = ratio of specific heats
δ = ratio of the thermal masses, gas/matrix, $r\rho c_p/\rho_m c_m$
ε = small dimensionless number, $d^2/4\alpha\tau$
η = efficiency
ρ = density of the cycle fluid
τ = period of revolution

Subscripts
L = corresponding to the left piston and/or heat source
m = regenerator matrix
R = corresponding to the right piston and/or heat sink
0 = leading-order term in perturbation series
1 = applied to x, interface left cylinder/regenerator
2 = applied to x, interface regenerator/right cylinder
11 = term of order ε in perturbation series
12 = term of order δ in perturbation series

Received Sept. 22, 1997; revision received Jan. 7, 1998; accepted for publication Jan. 8, 1998.

*Associate Professor, Department of Mechanical Engineering, 2500 University Drive NW. Member AIAA.

Introduction

THE near-isothermal regenerator model stems from an idea originally proposed by Rea and Smith[1] and Qvale and Smith,[2] implementing a perturbation analysis of the ideal Schmidt solution. A one-dimensional model was developed by Bauwens and extended to the general problem of oscillating flow in narrow tubes, with application to basic (nonorifice) pulse-tube refrigeration.[3–5] If the regenerator is well designed so that losses are small, the isothermal Schmidt model[6,7] is quite accurate, but predicts zero loss. The near-isothermal model adds a small perturbation to the Schmidt solution, which determines the losses resulting from nonideal heat transfer. While the original one-dimensional study[3] included evaluation of the enthalpy flux and a complete solution for temperature, a two-dimensional tubular pulse-tube study revealed that the enthalpy flux includes a reversible, thermoacoustic component, so that it is not equivalent to a heat leakage across the regenerator. Proper evaluation of the thermal loss in the regenerator requires a complete characterization of the higher-order heat engine, using a similar approach successfully used for the basic pulse-tube.[5]

The main source of entropy is heat transfer between the fluid and the matrix, which occurs across a small but finite temperature difference. This is accounted for in the energy equations in differential form (for the fluid and the matrix). In the global balance obtained by integrating both energy equations in time over one period and in space over the whole regenerator, and adding them up, the distinction between work and heat is no longer made. A different integration of the energy equations rewritten in entropy form yields the entropy production. While both integral laws are originally based upon the same field equations, complete characterization requires both global balances of energy and entropy.

This paper begins with the physical model followed by a summary of a previous study[3] that only included energy balance. Evaluation of the internal entropy production follows; thus extending to generic regenerator mesh topologies the approach used successfully in a pulse-tube study.[5] The loss associated with the entropy production is shown to result in small corrections to the external energy transfers because of a small pressure perturbation. A discussion of the issue of singular temperature profiles and a comparison with the Gifford and Longsworth profile[8,9] are included next. Finally, new results, including efficiency, are presented. Results from the current

one-dimensional model for generic mesh topologies, compared with two-dimensional ones for tubes, show that even when using the appropriate Nusselt number in the one-dimensional model they do not quite approach the correct limit.

Physical Model

The device, represented as spatially one-dimensional, is divided into cylinder spaces and the regenerator. The cylinders, including heat exchangers and dead volumes, are isothermal. The fluid is an ideal gas with constant specific heats. The sweep is of the same order as the regenerator length. The kinetic energy of the fluid is negligible. Pressure gradients are not dealt with in the current study. (For suitable magnitude assumptions, they can be formally decoupled. They can then be calculated from the mass flow rates, using an empirical friction model.[4] One can even show that, in contrast with the heat transfer problem discussed next, for viscous friction the empirical model is consistent.)

In one-dimensional models the actual details of the flow and the transverse gradients, which ultimately determine local heat transfer, are unavoidably lost. The standard approach was thus adopted to instead use an empirical convection model for heat transfer. In dimensionless form the convection coefficient appears as a Nusselt or Stanton number whose relationship with the Reynolds number and the Prandtl number is obtained from experiments. Whenever the problem is characterized by a single combination of a Nusselt number, a Reynolds number, and a Prandtl number, and provided that any other dimensionless parameters, such as geometric data, are included in the correlation, this approach is an unassailable consequence of dimensional analysis. In the regenerator problem the length scale characterizing the mesh is much smaller than all other lengths, and as a result, the time scale associated with local temperature adjustments is also shorter than global time scales such as the period. This would seem to justify reducing the local, instantaneous convection problem to a local, instantaneous Nusselt number, which, besides the Prandtl number that is constant, depends upon the local, instantaneous Reynolds number.

But local instantaneous heat transfer is characterized by a balance between transverse conduction in the fluid and ultimately with the matrix, and two sources of energy from the fluid, of equal magnitude: One obviously being convection because the flow brings in fluid at a temperature that differs from the local matrix temperature, but also because of pressure fluctuations. The first contribution occurs even at constant pressure and it is adequately represented by a Nusselt number that depends upon the Reynolds number. The second contribution is thermoacoustic in nature; it is independent of the flow motion and it occurs even at zero Reynolds number. Thus one should not expect that this second contribution will be adequately represented by a standard heat transfer correlation.

Still, for realistic topologies, resolving the actual details of the matrix and the flow is impossible. The one-dimensional model with heat transfer based upon local, instantaneous, Nusselt numbers is then the most sophisticated approach that is reasonably practical, even in numerical models.[7] The current study is based upon that approach. (In many cases, for example, first-order harmonic analysis, one is limited to simpler models. The best that can be done is to then use a constant value for the Nusselt number, based upon an average Reynolds number; an improvement presented by Kornhauser and Smith[10] is to use a complex-valued constant Nusselt number.) The two-dimensional near-isothermal solution for tubular geometries, in which the transverse gradients are accurately resolved, provides a reference solution that will be used as a benchmark, allowing for an assessment of the limitations of the empirical convection coefficient in the presence of pressure fluctuations.

The key dimensionless parameters are ε, the square of the ratio between matrix size and heat penetration depth, and the ratio δ of the thermal masses, of the fluid and the matrix. In contrast with a previous study,[3] in which they were assumed to be of the same magnitude, δ and ε are now assumed independent, as in the tube analysis,[4,5] which makes the results more general and facilitates the comparison. A third parameter, $\tau\alpha_m/L^2$, characterizing longitudinal conduction in the matrix, is of order $\varepsilon\delta$. The constant $a = \tau\alpha_m/\varepsilon\delta L^2$ is then of order unity.[3]

The longitudinal x coordinate is rescaled to represent volume rather than length. The Nusselt numbers are based upon actual areas and velocities and upon the size of the flow passages. The spatial domain is the interval $[x_L(t), x_R(t)]$. $x_L(t)$ and $x_R(t)$ describe the piston positions; they are known periodic functions of time. The expansion space is the volume between x_L and x_1 and the compression space, between x_2 and x_R. Finally, the regenerator is the space between the fixed locations x_1 and x_2. The problem is characterized by mass and energy conservation for the fluid and the energy equation for the matrix:

$$\frac{\partial \rho}{\partial t} + \frac{\partial \dot{m}}{\partial x} = 0 \tag{1}$$

$$\rho c_p \frac{\partial T}{\partial t} + c_p \dot{m} \frac{\partial T}{\partial x} - \frac{\mathrm{d}p}{\mathrm{d}t} = \frac{4\alpha\rho c_p Nu}{d^2}(T_m - T) \tag{2}$$

$$\rho_m c_m \frac{\partial T_m}{\partial t} = k_m \frac{\partial^2 T_m}{\partial x^2} + Nu \frac{4\alpha\rho c_p r}{d^2}(T - T_m) \tag{3}$$

The resulting dimensionless problem formulation is as follows: The problem is to find time-periodic solutions $\dot{m}(x, t)$, $p(t)$, $\rho(x, t)$, $T(x, t)$, and $T_m(x, t)$, in the interval $[x_L(t), x_R(t)]$, except for T_m, which is defined in $[x_1, x_2]$, satisfying Eqs. (4):

$$\frac{\partial \rho}{\partial t} + \frac{\partial \dot{m}}{\partial x} = 0 \tag{4a}$$

$$T = T_L(x) \quad \text{for} \quad x < x_1 \tag{4b}$$

$$T = T_R(x) \quad \text{for} \quad x > x_2 \tag{4c}$$

$$\varepsilon\left(\rho \frac{\partial T}{\partial t} + \dot{m} \frac{\partial T}{\partial x} - \frac{\gamma - 1}{\gamma} \frac{\mathrm{d}p}{\mathrm{d}t}\right) = Nu(T_m - T) \quad \text{for} \quad x \in (x_1, x_2) \tag{4d}$$

$$\varepsilon \frac{\partial T_m}{\partial t} = \varepsilon^2 \delta a \frac{\partial^2 T_m}{\partial x^2} + \delta Nu(T - T_m) \quad \text{for} \quad x \in (x_1, x_2) \tag{4e}$$

$$p = \rho T \tag{4f}$$

with boundary conditions

$$\dot{m}(x_L) = \rho(x_L) \frac{\mathrm{d}x_L}{\mathrm{d}t} \tag{4g}$$

$$\dot{m}(x_R) = \rho(x_R) \frac{\mathrm{d}x_R}{\mathrm{d}t} \tag{4h}$$

The piston positions x_L and x_R are known periodic functions of time with period 1. T_L and T_R are the known freezer and cooler temperatures, respectively. Nu is a function of the local, instantaneous Reynolds number. The total mass of fluid equals 1.

Solution

The basic solution has appeared elsewhere.[3] All variables, T, T_m, p, ρ, $\dot{m}$, and s, are expressed by perturbation series in ε and δ using the following notation, for example, T:

$$T = T_0 + \varepsilon T_{11} + \delta T_{12} + \varepsilon^2 T_{21} + \cdots \tag{5}$$

To leading order the indeterminate Schmidt solution $T_{m0} = T_0 = T_0(x)$ is obtained: For a matrix with infinite thermal mass and infinite heat transfer coefficient between fluid and matrix the temperatures never depart from their arbitrary initial value. Replacing density from $p_0 = \rho_0 T_0$ in leading-order continuity and integrating between x_L and x

$$\dot{m}_0 = -\frac{1}{T_L}\frac{\mathrm{d}[p_0(x_1 - x_L)]}{\mathrm{d}t} - \frac{\mathrm{d}p_0}{\mathrm{d}t}\int_{x_1}^{x}\frac{1}{T_0}\,\mathrm{d}x \tag{6}$$

While integrating from x_L to x_R, and with time

$$p_0 = 1\Big/\left(\frac{x_1 - x_L}{T_L} + \int_{x_1}^{x_1}\frac{1}{T_0}\,\mathrm{d}x + \frac{x_R - x_2}{T_R}\right) \tag{7}$$

Taking Eq. (6) into account, the components of order ε and δ of Eqs. (4d) and (4e) are readily solved, showing that $T_{m11} = T_{m11}(x)$, and

$$T_{11} = T_{m11}(x) - \frac{1}{Nu_0}\left(\dot{m}_0\frac{\mathrm{d}T_0}{\mathrm{d}x} - \frac{\gamma - 1}{\gamma}\frac{\mathrm{d}p_0}{\mathrm{d}t}\right) \tag{8}$$

$$T_{m12} = T_{12} = \frac{\gamma - 1}{\gamma}p_0 - \frac{\mathrm{d}T_0}{\mathrm{d}x}\int_0^t \dot{m}_0\,\mathrm{d}t \tag{9}$$

Adding the $\mathbb{O}(\varepsilon^2)$ perturbation to the energy equation for the fluid Eq. (4d), to the $\mathbb{O}(\varepsilon\delta)$ perturbation of the energy equation for the matrix Eq. (4e), a global energy balance is found. The time-derivative of the order δ^2 matrix temperature appears, which being periodic, vanishes when integrating over one full period

$$\frac{\mathrm{d}}{\mathrm{d}x}\int_0^1 \dot{m}_0 T_{11}\,\mathrm{d}t - a\frac{d^2T_0}{\mathrm{d}x^2} = 0 \tag{10}$$

Replacing T_{11} from Eq. (8), and integrating, the enthalpy flux appears as an integration constant

$$\dot{H}_{11} = \int_0^1 \frac{\dot{m}_0\,\mathrm{d}p_0}{Nu(Re_0)\,\mathrm{d}t}\,\mathrm{d}t - \frac{\gamma\,\mathrm{d}T_0}{\gamma - 1\,\mathrm{d}x}\int_0^1 \frac{\dot{m}_0^2}{Nu(Re_0)}\,\mathrm{d}t - a\frac{\gamma\,\mathrm{d}T_0}{\gamma - 1\,\mathrm{d}x} \tag{11}$$

And it is worth noting that there is an enthalpy flux of order δ also

$$\dot{H}_{12} = \frac{\gamma}{\gamma - 1}\int_0^1 \dot{m}_0 T_{12}\,\mathrm{d}t = \int_0^1 \dot{m}_0 p_0\,\mathrm{d}t \tag{12}$$

$\dot{H}_{11}$ and $\dot{H}_{12}$, which appear independently as absolute integration constants, are the largest contributions to the enthalpy flux because $\dot{H}_0 = 0$. Replacing $\dot{m}_0$ and p_0 by their expressions Eqs. (6) and (7), respectively, in Eq. (12), an ordinary differential equation for $T_0(x)$ is obtained, in which $\dot{H}_{11}$ plays the role of an eigenvalue.[3,4] [On the other hand $\dot{H}_{12}$ is constant for arbitrary profiles $T_0(x)$.] Except for $\dot{H}_{11} = 0$, no closed-form solution is found.[3,4]

Entropy Production

In the heat engine shown in Fig. 1 a heat source delivers a flux Q_L at temperature T_L and a heat sink dissipates a flux Q_R at T_R. Because $W_L - W_R = Q_L - Q_R$ for an engine, efficiency $\eta = (Q_L - Q_R)/Q_L$. Introducing the entropy fluxes $\dot{S}_L = Q_L/T_L$ and $\dot{S}_R = Q_R/T_R$, $\eta = 1 - (T_R/T_L)(\dot{S}_R/\dot{S}_L) = \eta_{\mathrm{CARNOT}} - (T_R/T_L)[(\dot{S}_R - \dot{S}_L)/\dot{S}_L]$. This expression, a direct consequence of the Gouy–Stodola theorem[11] and already known to Tolman and Fine,[12] allows for unconditional loss decoupling

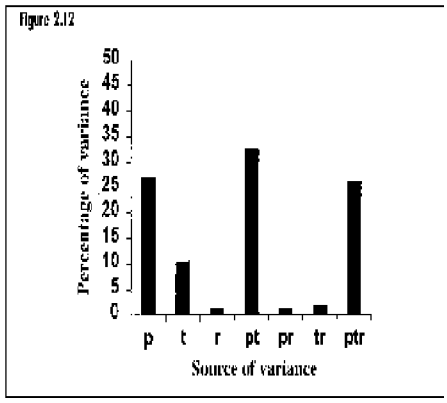

Fig. 1 Generic heat engine.

$$\eta = \eta_{\mathrm{CARNOT}} - \frac{T_R}{T_L}\frac{\Delta\dot{S}}{\dot{S}_L} \tag{13}$$

Unfortunately, in refrigerators, decoupling occurs for the inverse of the coefficient of performance (COP). Thus, one has to resort to magnitude arguments. The COP is given by $Q_L/(W_R - W_L) = Q_L/(Q_R - Q_L) = T_L/(T_R - T_L + T_R\Delta\dot{S}/\dot{S}_L)$. But in the case under study, the leading-order enthalpy flux is uniform and the correction of order δ is fully reversible, so that the larger order at which losses occur is ε; the COP is related to the entropy source $\Delta\dot{S}_{11}$:

$$\frac{\mathrm{COP}}{\text{Carnot COP}} = 1 - \varepsilon\frac{T_R}{T_R - T_L}\frac{\Delta\dot{S}_{11}}{\dot{S}_0} + \mathbb{O}(\varepsilon^2) \tag{14}$$

This provides an obvious motivation for evaluating $\Delta\dot{S}_{11}$, the entropy production. To that effect the energy equation, Eq. (4b), is converted to entropy form

$$\varepsilon\left(\rho T\frac{\partial s}{\partial t} + \dot{m}T\frac{\partial s}{\partial x}\right) = \frac{\gamma}{\gamma - 1}Nu(T_m - T) \tag{15}$$

Dividing by T, adding continuity Eq. (4a) times εs and integrating over a period, an expression for the spatial gradient of the entropy flux (the entropy created per unit length) is obtained, which, in contrast with the enthalpy flux, is not uniform lengthwise

$$\varepsilon\frac{\mathrm{d}\dot{S}}{\mathrm{d}x} = \frac{\gamma}{\gamma - 1}\int_0^1 Nu\,\frac{1}{T}(T_m - T)\,\mathrm{d}t \tag{16}$$

In view of Eq. (8) and $\dot{m}_0$ being periodic, the leading-order solution is isentropic and $\dot{S}_0$ is spatially uniform. Similarly, from Eq. (4e), so is $\dot{S}_{12}$, because the relevant perturbations to $Nu(T_m - T)$ are either zero or result in integration of a periodic expression. Similarly, for the component of order ε, from Eq. (4e), the perturbation of order $\varepsilon\delta$ to $Nu(T_m - T)$ is time-periodic and there is no leading-order temperature difference between the fluid and the gas. Thus

$$\frac{\mathrm{d}\dot{S}_{11}}{\mathrm{d}x} = -\frac{\gamma}{\gamma - 1}\frac{1}{T_0^2}\int_0^1 Nu_0 T_1(T_{m1} - T_1)\,\mathrm{d}t + a\frac{\gamma}{\gamma - 1}\frac{1}{T_0}\frac{d^2T_0}{\mathrm{d}x^2} \tag{17}$$

Equation (17) yields the entropy creation per unit length in the fluid. The irreversibility per unit length because of conduction in the matrix is given by

$$\frac{\mathrm{d}\dot{S}_{m11}}{\mathrm{d}x} = -a\,\frac{\gamma}{\gamma-1}\,\frac{d}{\mathrm{d}x}\left(\frac{1}{T_0}\,\frac{\mathrm{d}T_0}{\mathrm{d}x}\right) \tag{18}$$

Using Eqs. (6), (8), and (11), adding $\dot{S}_{11}$ and $\dot{S}_{m11}$ and integrating over the length

$$\Delta\dot{S}_{11} = \left(\frac{1}{T_R}-\frac{1}{T_L}\right)\dot{H}_{11} + \int_{x_1}^{x_2}\left\{\frac{d}{\mathrm{d}x}\left(\frac{1}{T_0}\right)\int_0^1 \frac{1}{Nu_0}\dot{m}_{0L}\frac{\mathrm{d}p_0}{\mathrm{d}t}\,\mathrm{d}t + \left[\frac{2\gamma-1}{\gamma}\frac{1}{T_0^2}-\frac{\mathrm{d}}{\mathrm{d}x}\left(\frac{1}{T_0}\int_{x_1}^{x}\frac{1}{T_0}\mathrm{d}x\right)\right]\int_0^1\frac{1}{Nu_0}\left(\frac{\mathrm{d}p_0}{\mathrm{d}t}\right)^2\mathrm{d}t\right\}\mathrm{d}x \tag{19}$$

in which all variables, $\dot{H}_{11}$, $T_0(x)$, $p_0(t)$, and $\dot{m}_0$, are known. $\Delta\dot{S}_{11}$ can now be evaluated, and Eq. (14) determines the drop in COP in relation to the Carnot limit. For constant Nu

$$\Delta\dot{S}_{11} = \left(\frac{1}{T_R}-\frac{1}{T_L}\right)\dot{H}_{11} + \frac{1}{Nu}\left(\frac{1}{T_R}\int_0^1 \dot{m}_{0R}\frac{\mathrm{d}p_0}{\mathrm{d}t}\,\mathrm{d}t - \frac{1}{T_L}\int_0^1\dot{m}_{0L}\frac{\mathrm{d}p_0}{\mathrm{d}t}\,\mathrm{d}t\right) + \frac{2\gamma-1}{Nu\gamma}\int_{x_1}^{x_2}\frac{1}{T_0^2}\,\mathrm{d}x\int_0^1\left(\frac{\mathrm{d}p_0}{\mathrm{d}t}\right)^2\mathrm{d}t \tag{20}$$

This results in a correction of $\mathcal{O}(\varepsilon)$ in the COP and in the external energy fluxes such as piston work and heat transfer. If W_{11L} and W_{11R} are the work of order ε on both extremities, with a positive sign corresponding to the work done by the spaces on the left on spaces on the right, then combining the first and second laws

$$\Delta\dot{S}_{11} - \left(\frac{1}{T_R}-\frac{1}{T_L}\right)\dot{H}_{11} = \frac{W_{11L}}{T_L} - \frac{W_{11R}}{T_R}$$

Because the piston motion is fully characterized by $x_L(t)$ and $x_R(t)$, $\mathcal{O}(\varepsilon)$ piston work requires a nonzero p_{11}

$$\Delta\dot{S}_{11} = \dot{S}_{11R} - \dot{S}_{11L} - \left(\frac{1}{T_R}-\frac{1}{T_L}\right)\dot{H}_{11} = \frac{W_{11L}}{T_L} - \frac{W_{11R}}{T_R} = \int_0^1 p_{11}\left(\frac{u_L}{T_L}-\frac{u_R}{T_R}\right)\mathrm{d}t \tag{21}$$

Thus, an alternate way to obtain the result of Eq. (19) is to find p_{11} and to evaluate this expression directly. p_{11} is determined from mass conservation of order ε

$$p_{11} = p_0^2\int_{x_1}^{x_2}\frac{T_{11}}{T_0^2}\,\mathrm{d}x \tag{22}$$

Comparison with Two-Dimensional Results

The one-dimensional model using empirical heat transfer is a necessary compromise when dealing with complex matrix topology. The associated cost can be evaluated using as a benchmark the two-dimensional laminar solution in tubes, which does not use convection coefficients.[4,5] In laminar steady flow in round tubes an exact derivation of the Nusselt number yields the constant value of 48/11 for uniform heat flux. Interestingly, the two-dimensional study yields expressions in which most coefficients match the ones obtained here when that value of Nu is used. Only these coefficients that become zero in the absence of pressure fluctuations differ: in the first term in Eq. (11) and the second term in Eq. (19) the correct value of the coefficient is 1/6 instead of 11/48. The coefficient of the last term in Eq. (19) is $(7\gamma - 3)/24\gamma$, instead of $(2\gamma - 1)/Nu\gamma = (22\gamma - 11)/48\gamma$. In the first case the error corresponds to a factor of 11/8 or approximately 37% and in the last one, between 11/8 ($\gamma = 1$) and 11/7 ($\gamma \to \infty$). For helium, $\gamma = 5/3$, the factor is 77/52, close to 50%.

Clearly, the one-dimensional model with empirical heat transfer coefficients is not exact. Previously, the error on temperatures and enthalpy flux had generally been found to be small, as long as the pressure (or volume) amplitude were not too high; but these studies did not examine the coefficient of performance, which is obviously crucial.[4,5] Indeed, while the enthalpy flux equations differ by one only coefficient, in the entropy sources the entire contribution not directly associated with the enthalpy flux is affected. In both cases the error approaches zero in the small-pressure amplitude limit. But whether actual results for realistic pressure ratios, which are normally not very high, differ significantly between the two models can only be determined by the numerical comparison presented next.

Relationship with Gifford and Longsworth's Isentropic Singular Profile

Singular solutions[3,13] are not of practical significance in the regenerator problem, but they are useful in diagnosing what is wrong with convection coefficients and the one-dimensional physical model. Indeed, this model results in an isentropic singular solution, identical to the Gifford and Longsworth's profile,[8,9] which is clearly physically incorrect. (In tubes a non-isentropic profile originally identified by Müller[14] and Rott[15] occurs.[14,16])

The current theory results in a singular profile if one of the pistons and heat exchangers, say, at the left end, is replaced by a rigid wall, in which case $x_L = x_1$ and $\dot{m}_{0L} = 0$, or if the motions of the pistons are in opposite phase and neglecting longitudinal conduction in the wall ($a = 0$). The mass flow rate $\dot{m}_0$ given by Eq. (6) becomes proportional to $(\mathrm{d}p_0/\mathrm{d}t)$. $\dot{H}_{11}$ is then necessarily zero because it is spatially uniform and equal to zero at $x = x_1$. Factoring the time integrals out of Eq. (11) a $1 - \gamma$ power-law solution is obtained, identical to Gifford and Longsworth's profile with $T_0 \to \infty$ at $x = 0$ and $T_{11} = 0$; hence, from Eq. (20), $\Delta\dot{S} = 0$.

Gifford and Longsworth's profile[8,9,13–16] requires a one-dimensional isentropic oscillating flow with negligible pressure gradients but large pressure fluctuations, to the right of a rigid wall located at $x = 0$. In this scenario there exists an entropy stratification in the fluid column such that its temperature profile remains steady and time independent. Indeed, consider a fluid parcel initially at the location $x = x_0$ when the pressure equals $p(0)$, and at $x(t)$ at time t when the pressure is $p(t)$. For each slice of fluid of thickness Δx, pV^γ = constant, and $p^{-\gamma}\Delta x$ is time independent. But volumes are proportional to positions; if for each slice $p^{-\gamma}\Delta x$ is time independent, for the layer obtained by stacking up all slices between 0 and x, so is the sum of all $p^{-\gamma}\Delta x$, equal to $p^{-\gamma}x$. Thus, pV^γ = constant holds for columns of arbitrary thickness and for arbitrarily entropy stratifications, and $p(t)x^\gamma = p(0)x_0^\gamma$. But the total mass of fluid between the wall at $x = 0$ and $x(t)$ is constant, so that

$$\int_0^x \rho(x',\,t)\,\mathrm{d}x' = \int_0^{x_0}\rho(x',\,0)\,\mathrm{d}x'$$

Replacing ρ from the ideal gas law and dividing by $p(t)x^\gamma = p(0)x_0^\gamma$

$$x_0^\gamma\int_0^x\frac{1}{T(x',\,t)}\,\mathrm{d}x' = x^\gamma\int_0^{x_0}\frac{1}{T(x',\,0)}\,\mathrm{d}x' \tag{23}$$

But Gifford and Longsworth's[9] solution requires temperatures that are time independent. Then $T(x, t) = T(x, 0) = T(x)$, and differentiating Eq. (23) with respect to x

$$x_0^{\gamma} \frac{1}{T(x)} = \gamma x^{\gamma-1} \int_0^{x_0} \frac{1}{T(x')}\, dx' \tag{24}$$

$x^{\gamma-1}T(x)$ is thus constant and a power law with exponent $1 - \gamma$ is obtained. In the absence of longitudinal conduction and for one-dimensional plug flow in a duct, this temperature profile is maintained even if the duct walls are not insulated from the fluid. Indeed, even then, as long as the wall temperature profile matches the profile in the fluid, no heat transfer will occur. This solution is thus entirely reversible and does not absorb any work.

Comparing the regenerator and Gifford and Longsworth models, transverse gradients are not resolved in either, and both lead to the same time-independent singular temperature profile. Unfortunately, this correspondence does not enhance the physical significance of either model. Indeed, there is no known physical process that results in the free half-space Gifford and Longsworth solution. Conversely, the singular profile in the regenerator is reversible only because of the artificialism of the empirical convection model. In reality, regardless of the mesh topology, oscillating boundary layers do not vanish. In the presence of a longitudinal temperature gradient in the wall or matrix, they result in instantaneous transverse temperature gradients; hence, irreversibilities and a nonisentropic profile such as, for tubular regenerators, the Müller/Rott profile. In summary, singular profiles do exist under the current assumptions, but they cannot be isentropic. The one-dimensional model incorrectly yields the Gifford and Longsworth exponent because the Nusselt number is not suitable for the balance between conduction transverse to the flow and pressure fluctuations. And for a different value of the dimensionless parameter the exact balance between pressure fluctuation and advection that characterizes the Gifford and Longsworth solution no longer occurs in the regenerator.

Numerical Results

To assess the impact of this inconsistency, a numerical study was carried out for realistic regenerators. Using a second-order-accurate procedure,[3,4] solutions were obtained for a constant Nusselt number, for helium $\gamma = 5/3$, both from the one-dimensional model and for a two-dimensional tubular regenerator for three configurations. ε and Nu (in one dimension) were kept as parameters. Longitudinal conduction was neglected ($a = 0$). For refrigerator no. 1 the amplitudes of the sinusoidal piston motion were equal to one-tenth of the void regenerator volume on the expansion side, and 2.2 times the regenerator volume on the compression side. With dead volumes to midstroke, respectively, equal to 0.11 and 2.4 times the regenerator volume, this was a high-volume ratio device, with the ratio maximum/minimum volume going from 5.61/1.41 for zero-phase angle to 5.81/1.21 at 180 deg. Refrigerator no. 2 featured displacements equal, respectively, to 0.05 and

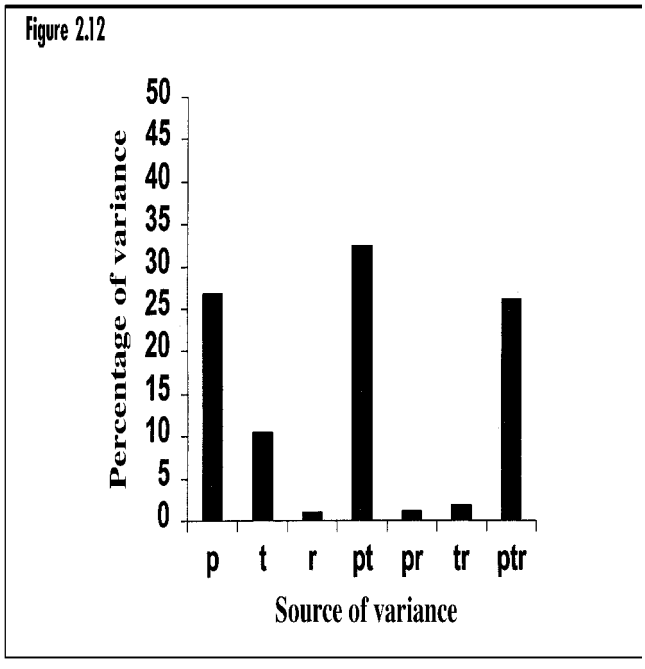

Fig. 2 Refrigerator no. 1, $(Nu/\varepsilon)[1 - (\text{COP/Carnot COP})]$ from the one-dimensional model.

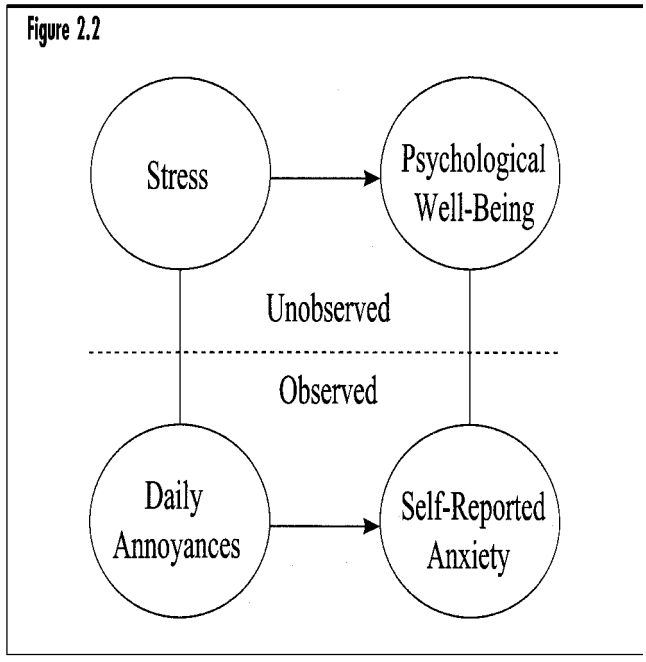

Fig. 3 Refrigerator no. 1, dimensionless refrigeration from the one-dimensional model.

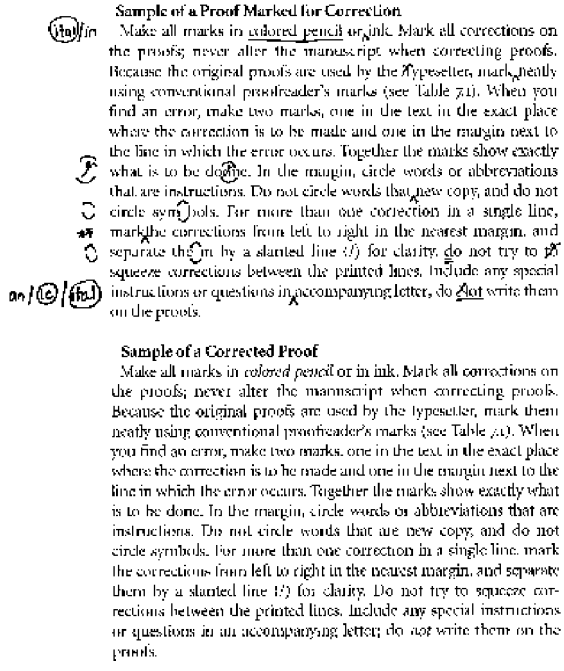
Sample of a Proof Marked for Correction

Make all marks in colored pencil or ink. Mark all corrections on the proofs; never alter the manuscript when correcting proofs. Because the original proofs are used by the typesetter, mark them neatly using conventional proofreader's marks (see Table 2.1). When you find an error, make two marks, one in the text in the exact place where the correction is to be made and one in the margin next to the line in which the error occurs. Together the marks show exactly what is to be done. In the margin, circle words or abbreviations that are instructions. Do not circle words that are new copy, and do not circle symbols. For more than one correction in a single line, mark the corrections from left to right in the nearest margin, and separate them by a slanted line (/) for clarity. do not try to squeeze corrections between the printed lines. Include any special instructions or questions in accompanying letter, do not write them on the proofs.

Sample of a Corrected Proof

Make all marks in *colored pencil* or in ink. Mark all corrections on the proofs; never alter the manuscript when correcting proofs. Because the original proofs are used by the typesetter, mark them neatly using conventional proofreader's marks (see Table 2.1). When you find an error, make two marks, one in the text in the exact place where the correction is to be made and one in the margin next to the line in which the error occurs. Together the marks show exactly what is to be done. In the margin, circle words or abbreviations that are instructions. Do not circle words that are new copy, and do not circle symbols. For more than one correction in a single line, mark the corrections from left to right in the nearest margin, and separate them by a slanted line (/) for clarity. Do not try to squeeze corrections between the printed lines. Include any special instructions or questions in an accompanying letter; do *not* write them on the proofs.

Fig. 4 Refrigerator no. 1, $(Nu/\varepsilon)[1 - (\text{COP/Carnot COP})]$ from the two-dimensional model.

1.1 and dead volumes of 0.055 and 1.2 times the regenerator volume, with volume ratios from 3.305/1.205 to 3.405/1.105. Finally, refrigerator no. 3 had displacements identical to refrigerator 2 and dead volumes equal to refrigerator no. 1, with volume ratios from 4.56/2.36 to 4.66/2.35.

Solutions were obtained for an array of phase angles between piston positions from 0 to 180 deg, in intervals of 5 deg, and temperature ratios from 0.025 to 1 in intervals of 0.025. Temperatures and enthalpy flux were determined from either Eq. (12) or its two-dimensional equivalent.[3,4] Entropy sources were evaluated from Eq. (23) or its equivalent.

Figures 2–5 show the results for refrigerator no. 1, Figs. 6–9 for refrigerator no. 2, and Figs. 10–13, for refrigerator no. 3. In each case the first two figures correspond to the one-

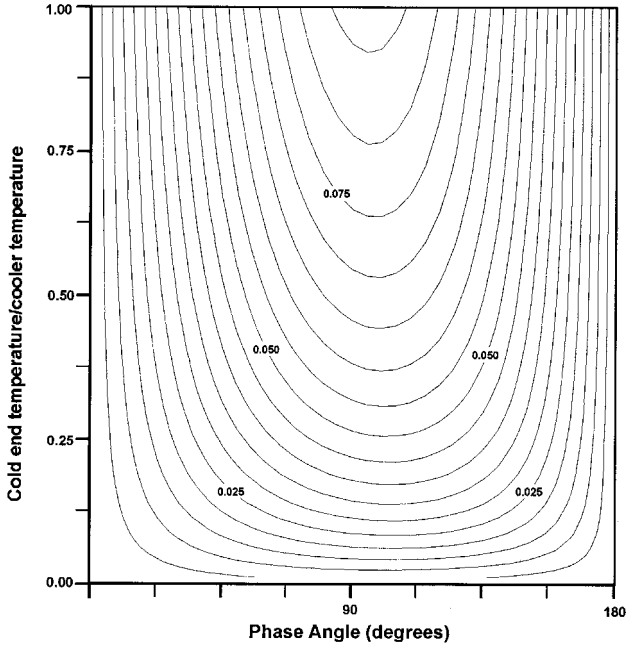

Fig. 5 Refrigerator no. 1, dimensionless refrigeration from the two-dimensional model.

Sample of a Proof Marked for Correction

Make all marks in colored pencil or ink. Mark all corrections on the proofs; never alter the manuscript when correcting proofs. Because the original proofs are used by the typesetter, mark neatly using conventional proofreader's marks (see Table 7.1). When you find an error, make two marks, one in the text in the exact place where the correction is to be made and one in the margin next to the line in which the error occurs. Together the marks show exactly what is to be done. In the margin, circle words or abbreviations that are instructions. Do not circle words that are new copy, and do not circle symbols. For more than one correction in a single line, mark the corrections from left to right in the nearest margin, and separate them by a slanted line (/) for clarity. Do not try to squeeze corrections between the printed lines. Include any special instructions or questions in accompanying letter; do not write them on the proofs.

Sample of a Corrected Proof

Make all marks in *colored pencil* or in ink. Mark all corrections on the proofs; never alter the manuscript when correcting proofs. Because the original proofs are used by the typesetter, mark them neatly using conventional proofreader's marks (see Table 7.1). When you find an error, make two marks, one in the text in the exact place where the correction is to be made and one in the margin next to the line in which the error occurs. Together the marks show exactly what is to be done. In the margin, circle words or abbreviations that are instructions. Do not circle words that are new copy, and do not circle symbols. For more than one correction in a single line, mark the corrections from left to right in the nearest margin, and separate them by a slanted line (/) for clarity. Do not try to squeeze corrections between the printed lines. Include any special instructions or questions in an accompanying letter; do *not* write them on the proofs.

Fig. 6 Refrigerator no. 2, (Nu/ε)[1 − (COP/Carnot COP)] from the one-dimensional model.

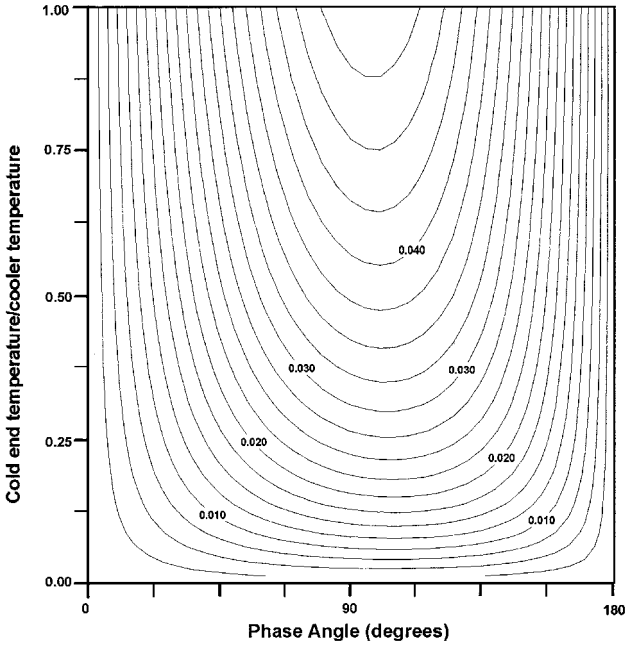

Fig. 7 Refrigerator no. 2, dimensionless refrigeration from the one-dimensional model.

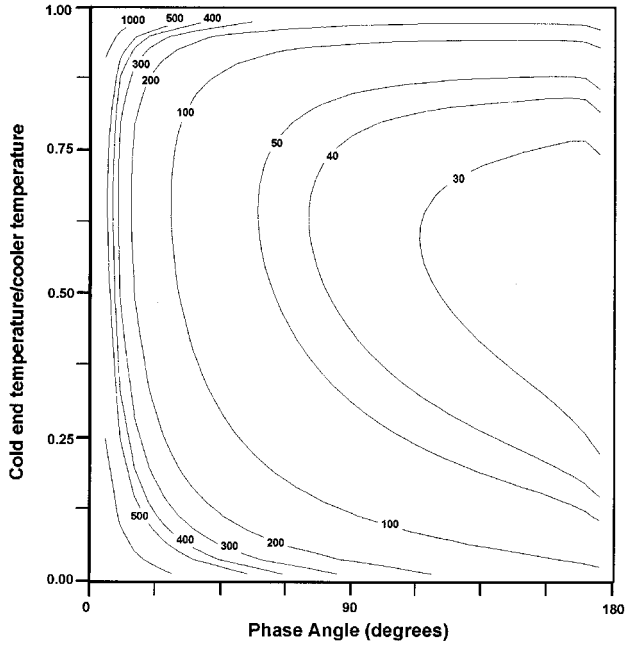

Fig. 8 Refrigerator no. 2, (Nu/ε)[1 − (COP/Carnot COP)] from the two-dimensional model.

dimensional model, and the last two to the two-dimensional model for tubes, reduced to a comparable form. The contour plots show, as functions of the phase shift between the two pistons and of the temperature ratio, the COP deficit × Nu/ε and the dimensionless refrigeration, respectively. The first quantity is

$$\frac{Nu}{\varepsilon}\left(1 - \frac{\text{COP}}{\text{Carnot COP}}\right)$$

and from Eq. (14) approximately equal to

$$Nu\,\frac{T_R}{T_R - T_L}\,\frac{\Delta \dot{S}_{11}}{\dot{S}_0}$$

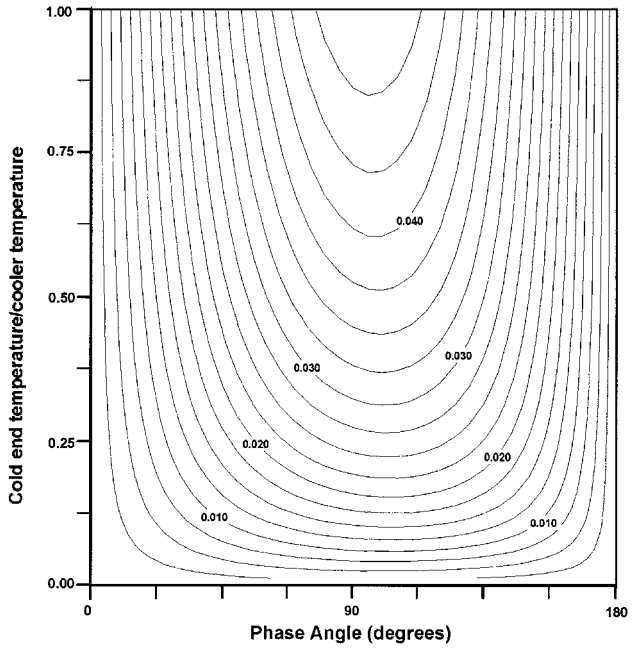

Fig. 9 Refrigerator no. 2, dimensionless refrigeration from the two-dimensional model.

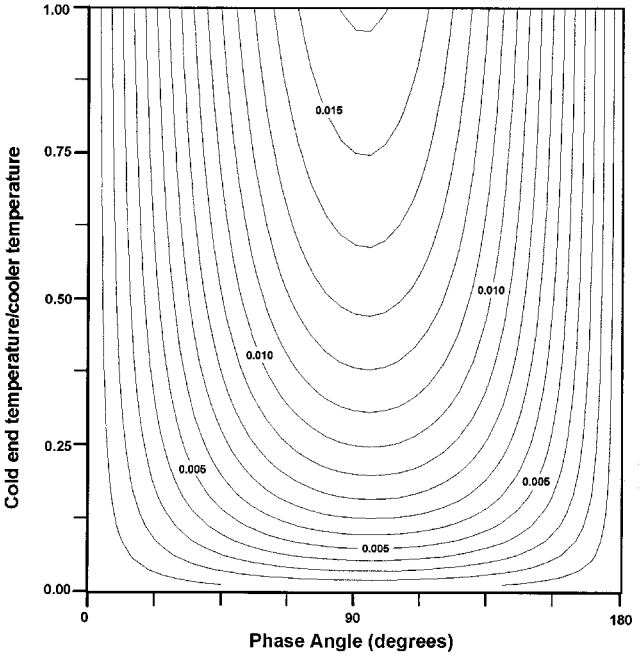

Fig. 11 Refrigerator no. 3, dimensionless refrigeration from the one-dimensional model.

Sample of a Proof Marked for Correction

Make all marks in pencil only (never in ink or black pencil). Mark all corrections on the proofs; never alter the manuscript when correcting proofs. Because the original proofs are used by the typesetter, mark them neatly using conventional proofreader's marks (see Table 14). When you find an error, make two marks, one in the text in the exact place where the correction is to be made and one in the margin next to the line in which the error occurs. Together the marks show exactly what is to be done. In the margin, circle words or abbreviations that are instructions. Do not circle words that are new copy, and do not circle symbols. For more than one correction in a single line, mark the corrections from left to right in the nearest margin, and separate them by a slanted line (/) for clarity. do not try to squeeze corrections between the printed lines. Include any special instructions or questions in accompanying letter; do Not write them on the proofs.

Sample of a Corrected Proof

Make all marks in *pencil only* (never in ink or in black pencil). Mark all corrections on the proofs; never alter the manuscript when correcting proofs. Because the original proofs are used by the typesetter, mark them neatly using conventional proofreader's marks (see Table 14). When you find an error, make two marks, one in the text in the exact place where the correction is to be made and one in the margin next to the line in which the error occurs. Together the marks show exactly what is to be done. In the margin, circle words or abbreviations that are instructions. Do not circle words that are new copy, and do not circle symbols. For more than one correction in a single line, mark the corrections from left to right in the nearest margin, and separate them by a slanted line (/) for clarity. Do not try to squeeze corrections between the printed lines. Include any special instructions or questions in an accompanying letter; do *not* write them on the proofs.

Fig. 10 Refrigerator no. 3, $(Nu/\varepsilon)[1 - (\text{COP}/\text{Carnot COP})]$ from the one-dimensional model.

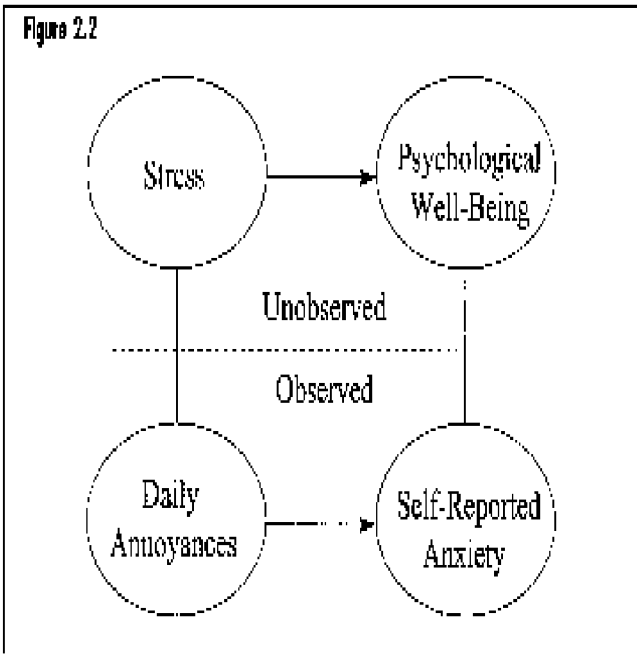

Fig. 12 Refrigerator no. 3, $(Nu/\varepsilon)[1 - (\text{COP}/\text{Carnot COP})]$ from the two-dimensional model.

is the expression most closely related to the COP that can be determined, while keeping Nu and ε as parameters. The second quantity, refrigeration, has been scaled by the product mass of fluid times frequency, times the gas constant, times the cooler temperature. [Once the mean temperature profile $T_0(x)$ is known complete results can be obtained, diagrams such as pressure–volume diagrams can be constructed, and all energy fluxes can be calculated. Additional regenerator losses such as viscous losses can also be evaluated.]

Overall the results show regenerator losses decreasing for increasing phase angle, although, for phase angles too close to 180 deg to show up on the plots, the two-dimensional model results in losses rapidly increasing with the phase angle. This is because, at the phase angle of 180 deg, an internal temperature singularity occurs of the type described in a previous section. Because the one-dimensional singular profile is isentropic, the loss approaches zero. But the two-dimensional singular solution is not isentropic; then, the entropy sources of order ε approach a finite limit, while the leading-order entropy flux approaches zero, so that the COP deficit tends to infinity at 180 deg.

At a given phase angle the COP deficit reaches a minimum value for some intermediate temperature ratio, which decreases for increasing phase angle and which is higher in the results based upon the two-dimensional model, and also, at a lower pressure ratio. As to the influence of dead volumes and pressure ratios, it is interesting to note that going from configu-

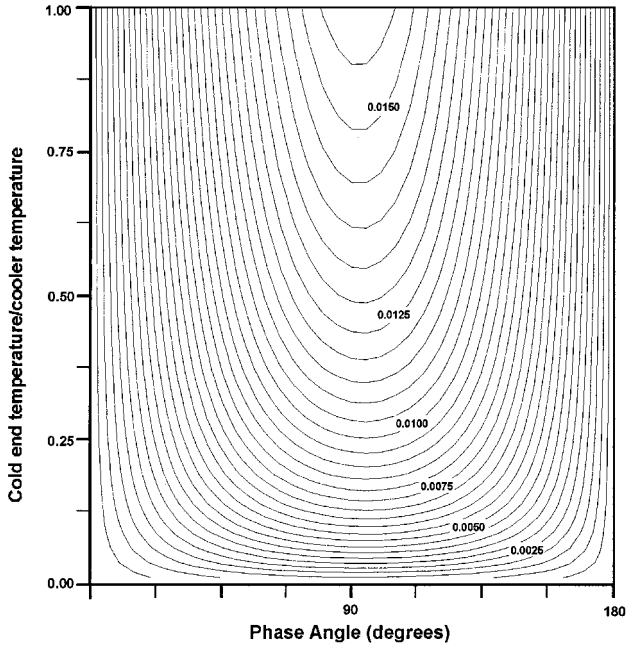

Fig. 13 Refrigerator no. 3, dimensionless refrigeration from the two-dimensional model.

ration no. 1 to no. 2, the regenerator loss actually increased, while it decreased from both designs no. 1 and no. 2 to design no. 3. Thus, lowering the pressure ratio through an increase in cylinder dead volume can result in lower thermal losses than if increasing the regenerator volume (even without considering friction or adiabatic losses).

Lowering the pressure amplitude obviously lowers the specific refrigeration. In all cases, refrigeration peaks at a phase angle somewhat larger than 90 deg, even though being a leading-order quantity, refrigeration is fully determined by the leading-order Schmidt model. This is because pressure was calculated taking into account the actual regenerator temperature profile based upon the complete solution, which varies with temperature ratio and phase angle. In contrast, usual Schmidt analysis assumes a constant, arbitrary temperature profile, which results in charts symmetrical about the 90-deg line.

Finally, as expected, the results from the one-dimensional model using empirical Nusselt numbers differ from the exact two-dimensional results obtained for tubular regenerators, and the difference is less pronounced as the volume amplitude is reduced. The results show a large error for refrigerator no. 1, when the pressure amplitude is large. While smaller, the difference in the COP deficit does not become insignificant at the smaller amplitudes corresponding to nos. 2 and 3. Except for phase angles near 180 deg, which are largely irrelevant in practice, the error is apparently always on the conservative side. The error in the predicted refrigeration in nos. 2 and 3 is only noticeable at low-temperature lift.

Because the Nusselt number model is correct insofar as the balance between advection and transverse heat transfer is concerned, but not when dealing with pressure fluctuations in Eqs. (11) and (19), one might want to introduce another, new dimensionless parameter to replace Nu in the first term of Eq. (11). That number characterizes the balance between isothermal pressure fluctuations and transverse heat transfer. This will require, however, a good fundamental justification and an adequate procedure for experimental determination. While this is a natural extension of the near-isothermal solution, a similar approach would not be feasible in true, direct numerical solutions to Eqs. (1–3), which do not distinguish between the two sources of energy. Finally, it is worth noting that similar conclusions could be reached also using the linearized small-amplitude model.[17]

Conclusions

The Schmidt model leaves the temperature profile indeterminate. Near-isothermal theory is powerful enough to determine not only the mean regenerator temperature profile and, hence, the correct pressure history, but also the detailed space- and time-dependent temperature fluctuations. The enthalpy flux, associated thermoacoustic effects, and entropy sources are then readily evaluated, and full characterization of the thermal performance is obtained, including the efficiency loss as a result of irreversibilities in the regenerator.

This study was based upon the same one-dimensional physical model implemented in most fully numerical solutions, using empirical correlations for convective heat transfer. While the Nusselt number was shown to represent correctly the balance between advection and exchange with the matrix, the effect of pressure fluctuations requires a different dimensionless parameter; otherwise, the results are physically inconsistent. In some cases the error was found to be numerically significant, even at realistically low-volume ratios. But this error is rooted in the inadequacy of the physical model, not in the solution technique, which, overall is arguably better than a full numerical approach, particularly because it could easily incorporate a more correct measure of the effect of pressure fluctuations, which full numerical solutions cannot handle.

Near-isothermal theory yields full regenerator performance characterization, including specific refrigeration, and COP at a reasonable cost. Trends are generally accurately predicted, and even if the magnitude of the error reaches the 30–50% range for the COP deficit the results remain useful, with an error probably well within the range of uncertainty because of uncertainties on the input data.

References

[1]Rea, S. N., and Smith, J. L., Jr., "The Influence of Pressure Cycling on Thermal Regenerators," *Journal of Engineering for Industry*, Series B, Vol. 89, No. 3, 1967, pp. 563–569.

[2]Qvale, E. B., and Smith, J. L., Jr., "An Approximate Solution for the Thermal Performance of a Stirling-Engine Regenerator," *Journal of Engineering for Power*, Series A, Vol. 91, No. 2, 1969, pp. 109–112.

[3]Bauwens, L., "Near-Isothermal Regenerator: A Perturbation Analysis," *Journal of Thermophysics and Heat Transfer*, Vol. 9, No. 4, 1995, pp. 749–756.

[4]Bauwens, L., "Oscillating Flow of a Heat-Conducting Fluid in a Narrow Tube," *Journal of Fluid Mechanics*, Vol. 324, 1996, pp. 135–161.

[5]Bauwens, L., "Entropy Balance and Performance Characterization of the Narrow Basic Pulse-Tube Refrigerator," *Journal of Thermophysics and Heat Transfer*, Vol. 10, No. 4, 1996, pp. 663–671.

[6]Schmidt, G., "Theorie der Lehmann'schen kalorische Maschine," *Zeitschrift des Vereins Deutscher Ingenieure*, Vol. 15, No. 1, 1871, pp. 1–9.

[7]Urieli, I., and Berchowitz, D. M., *Stirling Engine Analysis*, Hilger, Bristol, England, UK, 1984.

[8]Gifford, W. E., and Longsworth, R. C., "Pulse-Tube Refrigeration," *Journal of Engineering for Industry*, Series B, Vol. 86, No. 2, 1964, pp. 264–268.

[9]Gifford, W. E., and Longsworth, R. C., "Surface Heat Pumping," *Advances in Cryogenic Engineering*, Vol. 11, 1966, pp. 171–179.

[10]Kornhauser, A. A., and Smith, J. L, Jr., "Application of a Complex Nusselt Number to Heat Transfer During Compression and Expansion," *Journal of Heat Transfer*, Vol. 116, No. 3, 1994, pp. 536–542.

[11]Bejan, A., "Entropy Generation Minimization: The New Thermodynamics of Finite-Size Devices and Finite-Time Processes," *Journal of Applied Physics*, Vol. 79, No. 3, 1996, pp. 1191–1218.

[12]Tolman, R. C., and Fine, P. F., "On the Irreversible Production of Entropy," *Reviews of Modern Physics*, Vol. 20, No. 1, 1948, pp. 51–77.

[13]Bauwens, L., "Thermoacoustics: Transient Regimes and Singular Temperature Profiles," *Physics of Fluids*, Vol. 10, No. 4, 1998, pp. 807–818.

[14]Müller, U. A., "Thermoakustische Gasschwingungen: Definition und Optimierung eines Wirkungsgrades," Ph.D. Dissertation, Eidgenössische Technische Hochschule, Zürich, Switzerland, 1982.

[15]Rott, N., "Thermoacoustic Heating at the Closed End of an Oscillating Gas Column," *Journal of Fluid Mechanics*, Vol. 145, 1984, pp. 1–9.

[16]Wheatley, J., Hofler, T., Swift, G. W., and Migliori, A., "An Intrinsically Irreversible Thermoacoustic Heat Engine," *Journal of the Acoustical Society of America*, Vol. 74, No. 1, 1983, pp. 153–170.

[17]Swift, G. W., "Thermoacoustic Engines," *Journal of the Acoustical Society of America*, Vol. 84, No. 4, 1988, pp. 1145–1180.